9950-520

DOE/JPL
Distribution Category UC-63
Report #7

EBIC AND HVTEM STUDIES OF RTR SILICON RIBBON

April 1981

JPL Contract No. 954852

by

B. Cunningham, H. Strunk* and D. Ast

The JPL low-cost solar array project is sponsored by the U.S. Department of Energy and forms part of the Solar Photovoltaic Conversion Program to initiate a major effort toward the development of low-cost solar arrays. This work was performed for the Jet Propulsion Laboratory, California Institute of Technology by agreement between NASA and DOE.

*Present address: Max Planck Institut für Metallforschung, Institut für Physik, 7000 Stuttgart 80, FRG.

Abstract

The defect structure of RTR ribbon #6-731, run 803 was studied by CTEM, EBIC and HVTEM. Prior to laser recrystallization the defect structure consists of closely spaced twin and grain boundaries. Precipitation of impurities occurs after laser recrystallization. The observation of electrically active defects in EBIC has been correlated with HVTEM studies "Pairs" of electrically active defects in twin boundaries are due to stacking faults connecting the twin boundaries.

1. Introduction

The following study supplements work previously performed on RTR material, sample identification #6-731, run 803 /1/. The additional studies, carried out on specimens prepared during the original reporting period are: (1) TEM examination of the CVD (chemical vapor deposition) polycrystalline substrate prior to laser recrystallization (2) EBIC studies of the recrystallized substrate and (3) correlation between EBIC and HVTEM observations. A summary of the results presented in Report #4, JPL Contract #954852 "Defect Structure of RTR Silicon Ribbon" will also be given.

2. Previous Work

Table 1 summarizes the defect structure data previously determined by conventional TEM /1/. The high density of precipitates, due presumably to contamination from the Mo substrate used for CVD, was thought to be responsible for the low reported efficiencies of RTR silicon ribbons /2/. In addition, high densities of dislocations and stacking fault loops were observed. Attempts to image these specimens by EBIC (electron beam-induced current) microscopy were unsuccessful. The difficulties encountered in preparing good Schottky diodes were attributed to the high density of precipitates. An interesting observation in the previous study was that the dislocations were not decorated by precipitates. It was proposed therefore that the lattice dislocations were formed after the precipitation process, possibly after the annealing treatment.

3. Experimental Techniques

Scanning electron microscopy in the EBIC mode /3/ was used to characterize the local electrical properties i.e. the minority carrier recombination, at the defects. High voltage transmission electron microscopy (HVTEM) was used to determine the geometrical nature of defects previously imaged by EBIC. Conventional transmission electron microscopy (CTEM) was used to characterize the CVD substrate prior to laser recrystallization.

4. Results

a) TEM Studies of CVD Polycrystalline Silicon Substrate

Figure 1 shows a typical micrograph of the CVD silicon substrate. A large number of closely spaced twin and grain boundaries is observed but only a few lattice dislocations. The most significant observation is the absence of precipitates. The polycrystalline silicon is deposited on a molybdenum substrate which is known to introduce large quantities of Mo into the silicon /4/. This effect should be pronounced in the material used in the present study since no SiO_2 or Si_3N_4 diffusion barrier was used between the Mo substrate and the silicon.

b) EBIC Studies

Although a Schottky diode suitable for EBIC was eventually fabricated on the recrystallized RTR silicon, the quality and resolution were not as good as specimens prepared from other ribbons (e.g. EFG).

Figure 2(a) shows a typical EBIC micrograph from the RTR ribbon. Note that the image is very "noisy". A higher magnification micrograph, Figure 2(b), of the area delineated in Figure 2(a) shows that the horizontal lines are traces of twin or microtwin boundaries and that the EBIC contrast arises from electrically active dislocations in the boundary. There are also a large number of electrically active defects in the matrix material.

c) Correlation of EBIC and HVTEM

The correlation of EBIC and HVTEM requires that the same area be imaged by both techniques. Specimens are mapped out in EBIC and ion milled from the back side until the regions of interest are contained in the electron transparent areas. The present correlation was only partly successful in that the resolution of the EBIC micrographs was not high enough to facilitate an exact 1:1 correspondence with individual dislocations observed in the HVTEM.

Figure 3 shows an EBIC micrograph of active defects distributed along twin boundaries. Part of the area indicated in Figure 3 was imaged by HVTEM, Figure 4.

The twin boundaries are visible through fringe contrast in Figure 4(a). Although the EBIC and HVTEM micrographs cannot be exactly matched one can nevertheless conclude that the density of active defects observed in EBIC is lower than the density of dislocations observed in HVTEM. This observation implies that not all of the dislocations are electrically active.

From HVTEM three distinct dislocation types can be distinguished. (1) Dislocations with no precipate decoration (2) dislocations decorated with precipitates and (3) dislocations pinned by precipitates. Examples of each of these are shown in Figures 5(a)-5(c) respectively

Figure 6 shows HVTEM micrographs of stacking faults connecting the two twin boundaries. The stacking faults are out of contrast in Figure 6(b) and the bounding dislocations can be seen. Although the overlapping fringes from the two faults makes it difficult to determine their nature it seems likely that one is intrinsic and one extrinsic. This arrangement preserves the stacking sequence on either side of the faults. Figure 7 is an EBIC micrograph of "pairs" of active defects along the twin boundary imaged in Figure 6. In view of the HVTEM results we propose that the "pairing" is caused by stacking faults between the twin planes and that the contrast is due to the active partials which bound these stacking faults.

5. Discussion

Since no precipitates are observed in the ribbons prior to laser recrystallization, it is reasonable to assume that preferential diffusion takes place along the twin and grain boundaries and that diffusion into the matrix material is limited (during CVD process). During recrystallization the Mo is precipitated out into the matrix. Previous observations /1/ that the lattice dislocations were not decorated by precipitates and that the precipitation process occurs prior to dislocation generation are supported to a certain extent by the present studies. Several dislocations however are decorated, suggesting that some must be generated prior or concommitantly with the precipitation process.

There is indirect evidence that the electrical activity of dislocations depends on the temperature at which they are formed /5/. Formation of dislocations in two temperature regimes (laser recrystallization, post anneal) could therefore explain the observed variability in electrical activity (and also precipitation) at dislocations.

The presence of connecting twins and stacking faults and the corresponding EBIC observations of "pairs" of electrically active defects are interesting fault combinations which also contribute to the reduced efficiencies in RTR ribbons.

References

1. H. Strunk and D. Ast "Defect Structure of RTR Ribbons" JPL Technical Report #4, Contract #954852 (1980).

2. H.I. Hoo, P.A. Iles and D.P. Tanner "Silicon Solar Cell Process Development, Fabrication and Analysis", JPL Technical Report, Contract #955084 Optical Coating Laboratory (1979).

3. H.J. Leamy, L.C. Kimerling and S.D. Ferris, Scanning Electron Microsc., 1, 717 (1978).

4. K.R. Sarma, R.N. Legge and R.W. Gurtler, J. Electronic Materials 9, 841 (1980).

5. H. Strunk, B. Cunningham and D. Ast "Defect Structure of EFG Silicon Ribbon" JPL Technical Report #6, Contract #954852 (1980).

Figure Captions

1. Typical array of twin and grain boundaries in CVD polycrystalline silicon prior to laser recrystallization.
2. (a) EBIC micrograph showing electrical activity along twin boundaries in laser recrystallized RTR silicon.

   (b) Higher magnification EBIC micrograph of area shown in (a).
3. EBIC micrograph of electrically active defects in twin boundaries.
4. HVTEM micrographs of part of the area shown in EBIC micrograph of Figure 3. $\underline{g}$: diffraction vector.
5. HVTEM micrographs showing degrees of precipitation at dislocations (a) "clean" dislocations (b) decorated dislocations (c) pinned dislocations.
6. HVTEM micrographs of stacking faults connecting twin boundaries (a) stacking faults in contrast (b) twin boundaries in contrast.
7. EBIC micrograph of "pairs" of electrically active defects.

Table 1

Defect structure data extracted from TEM

Defect type	Density	Size	Remarks
dislocations	10^6 - 10^7 cm^{-2}	----	Density varies locally. No decoration by precipitates observed.
stacking faults	10^{10} cm^{-3}	3 µm ∅	Density estimated from investigated volume. Order of magnitude only.
twinned regions	----	thickness typ. 5-100 nm frequent length up to order of mm	Twins ending in matrix infrequent.
precipitates	1.2 x 10^{13} cm^{-3}	typ. 10-20 nm wide ~5 nm thick	Quasi-homogeneously distributed in the ribbon.

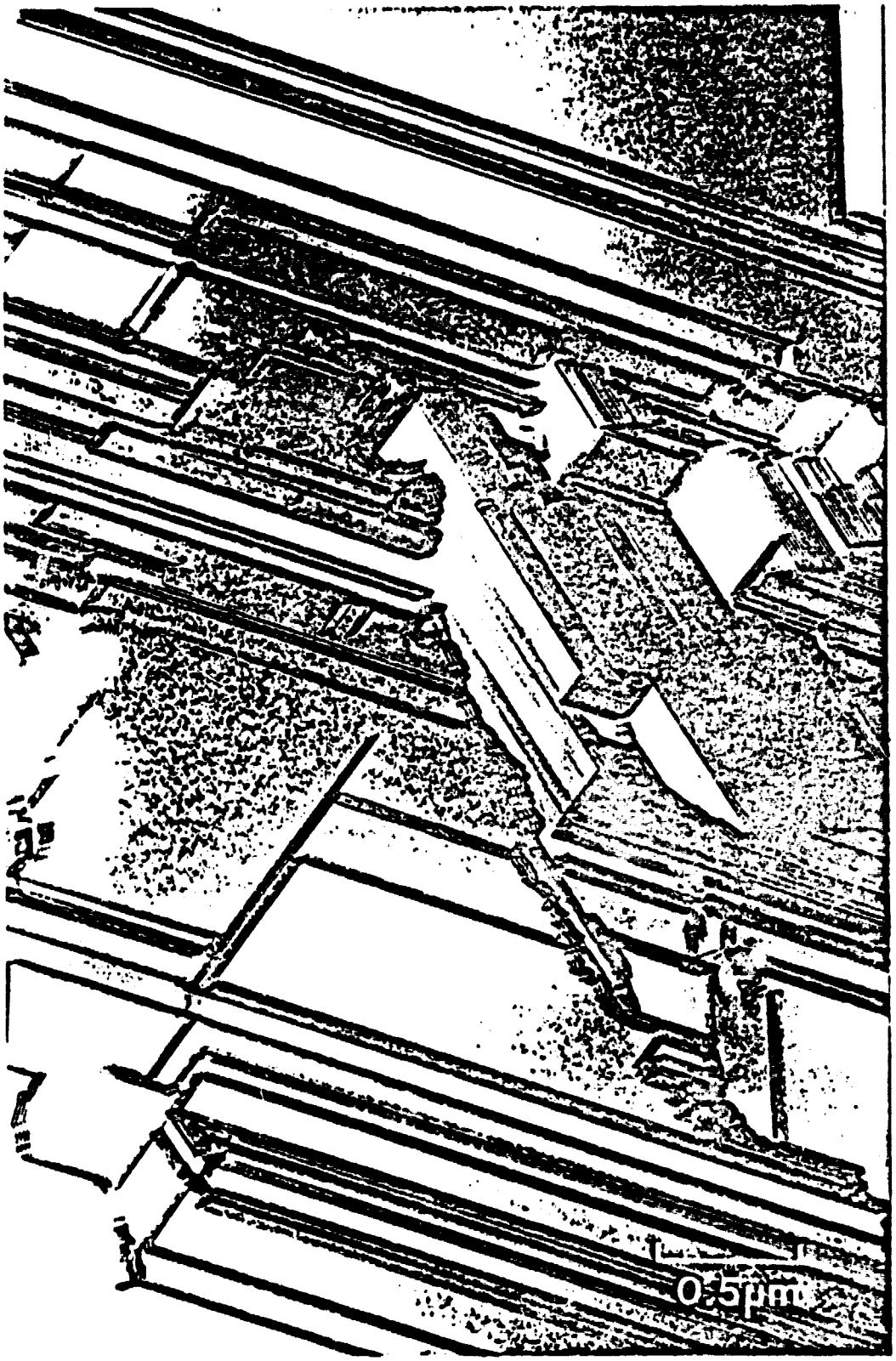

Figure 1

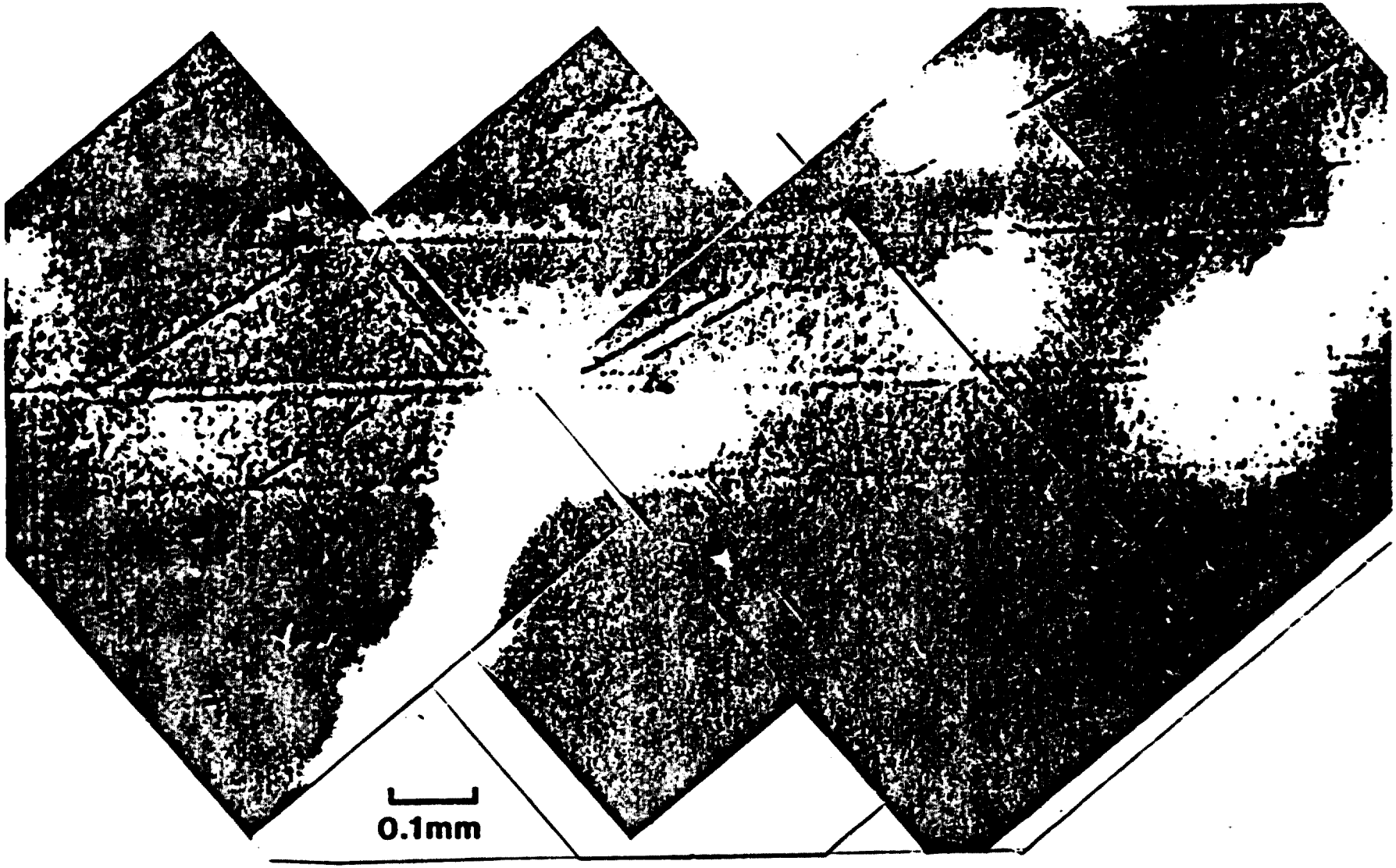

Figure 2(a)

Figure 2(b)

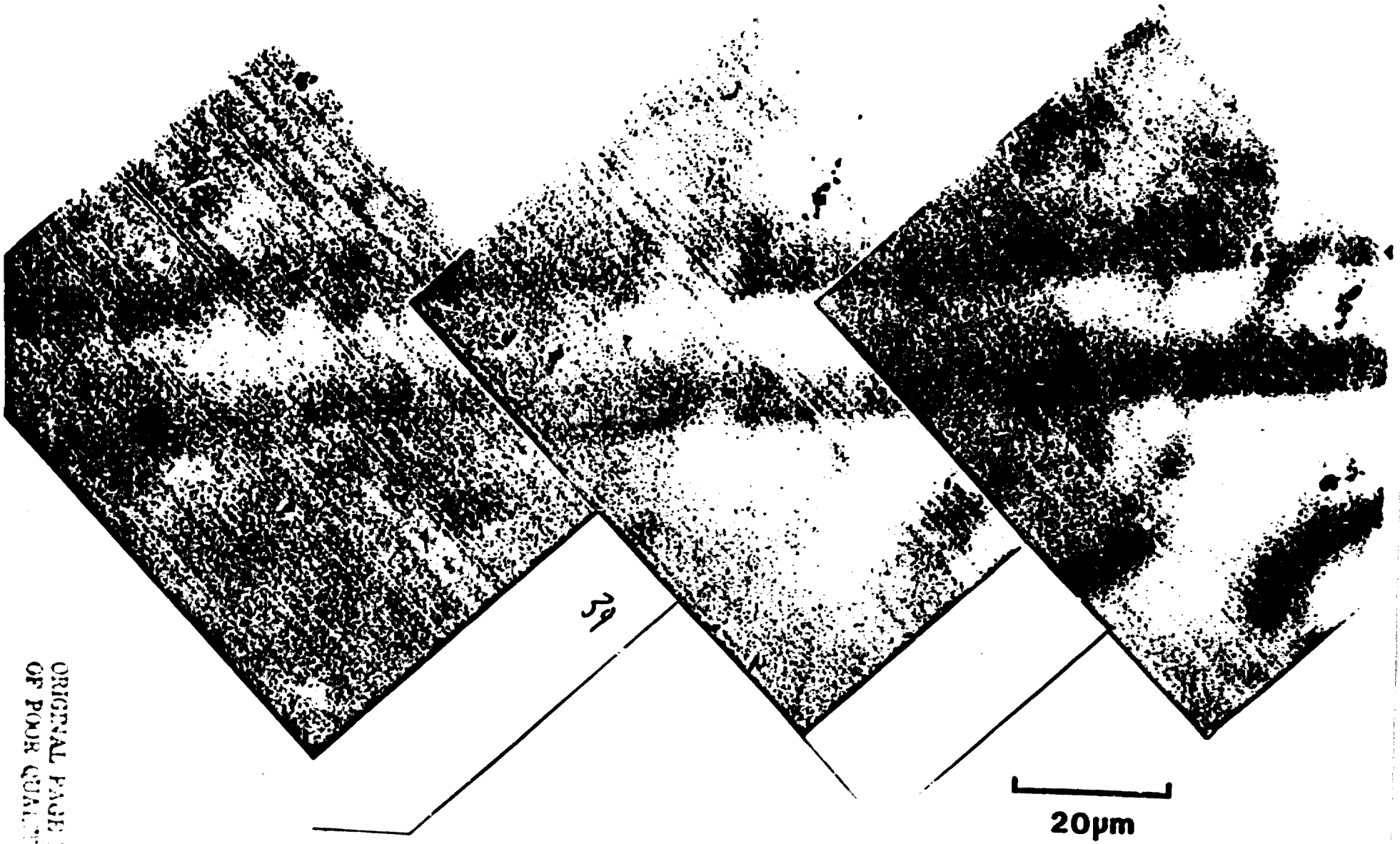

Figure 3

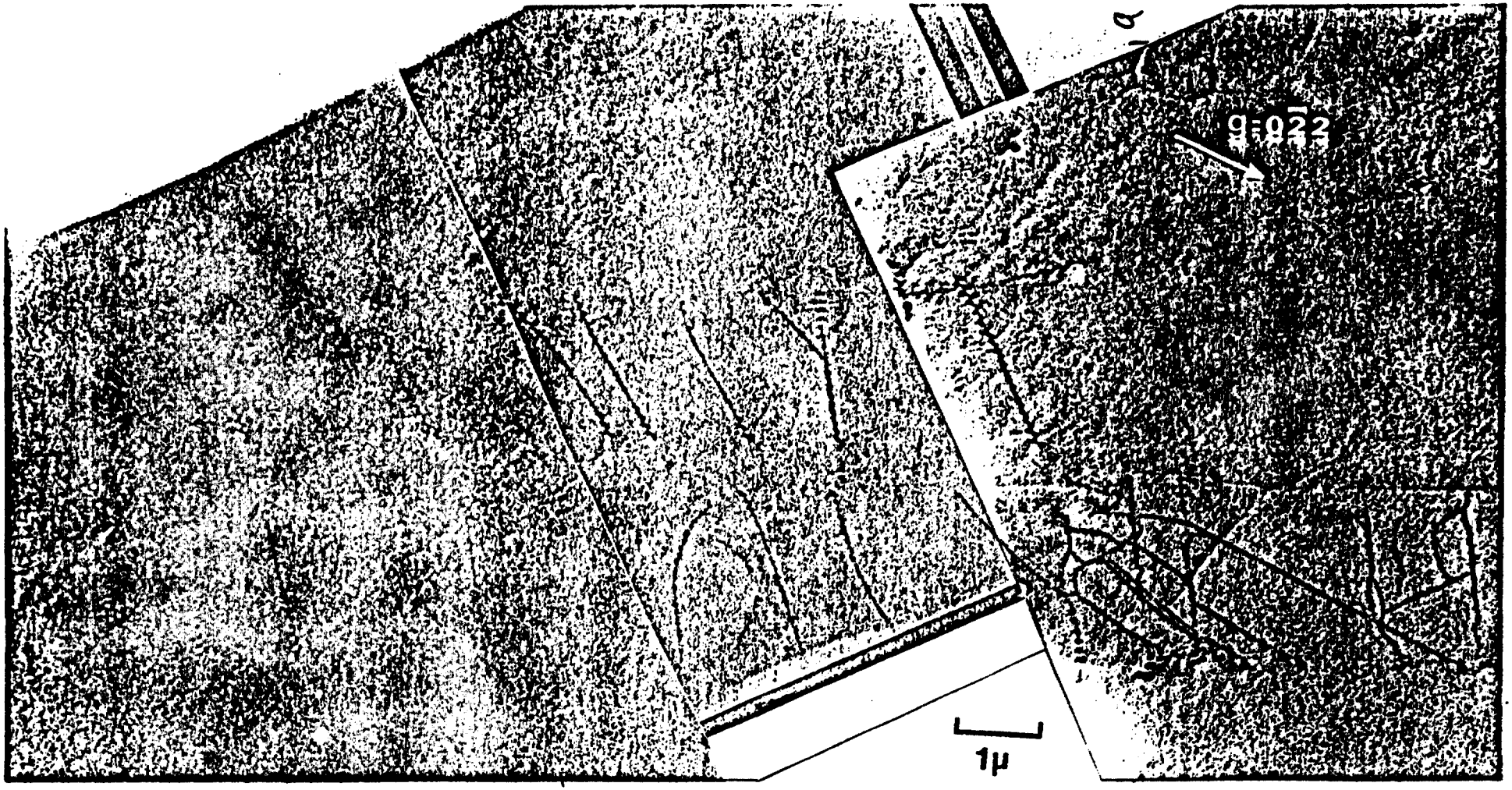

Figure 4

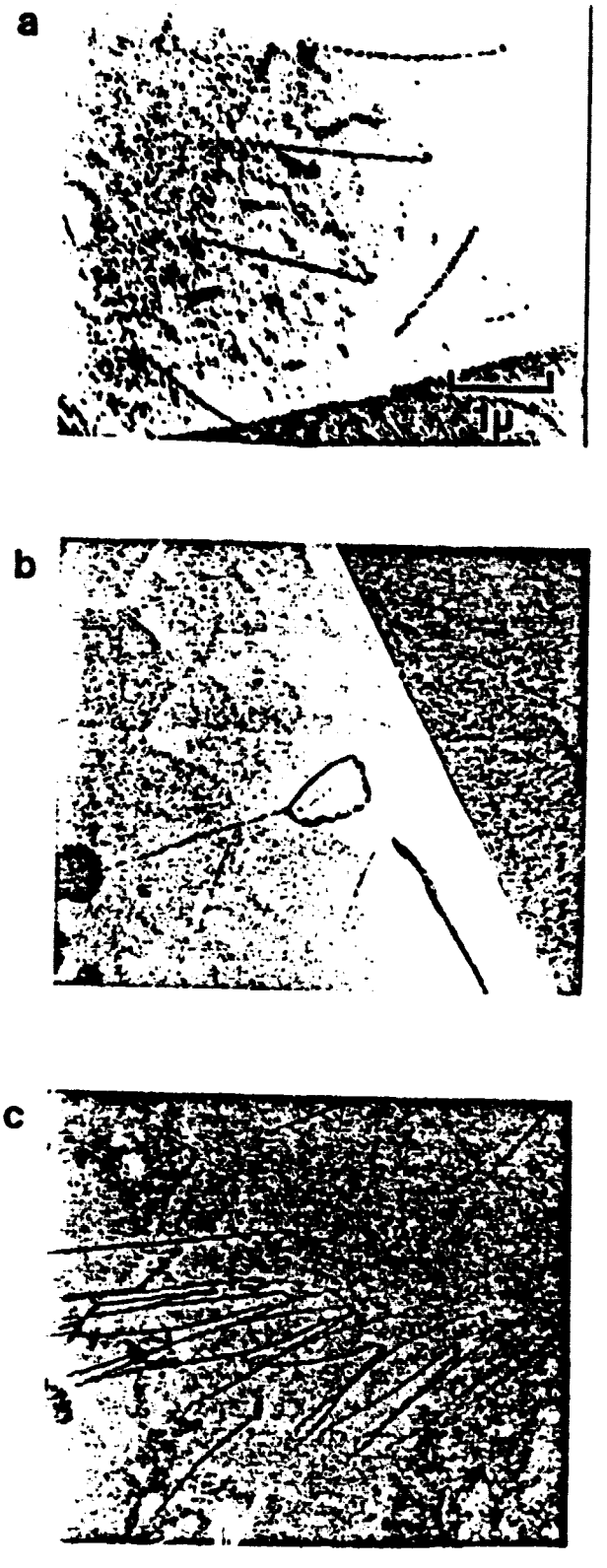

Figure 5

a

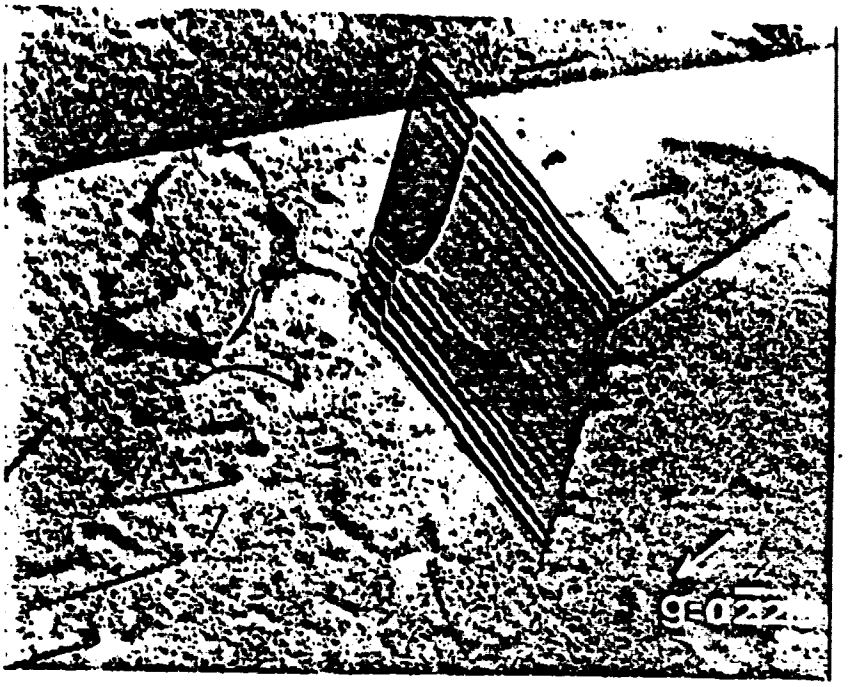

b

Figure 6

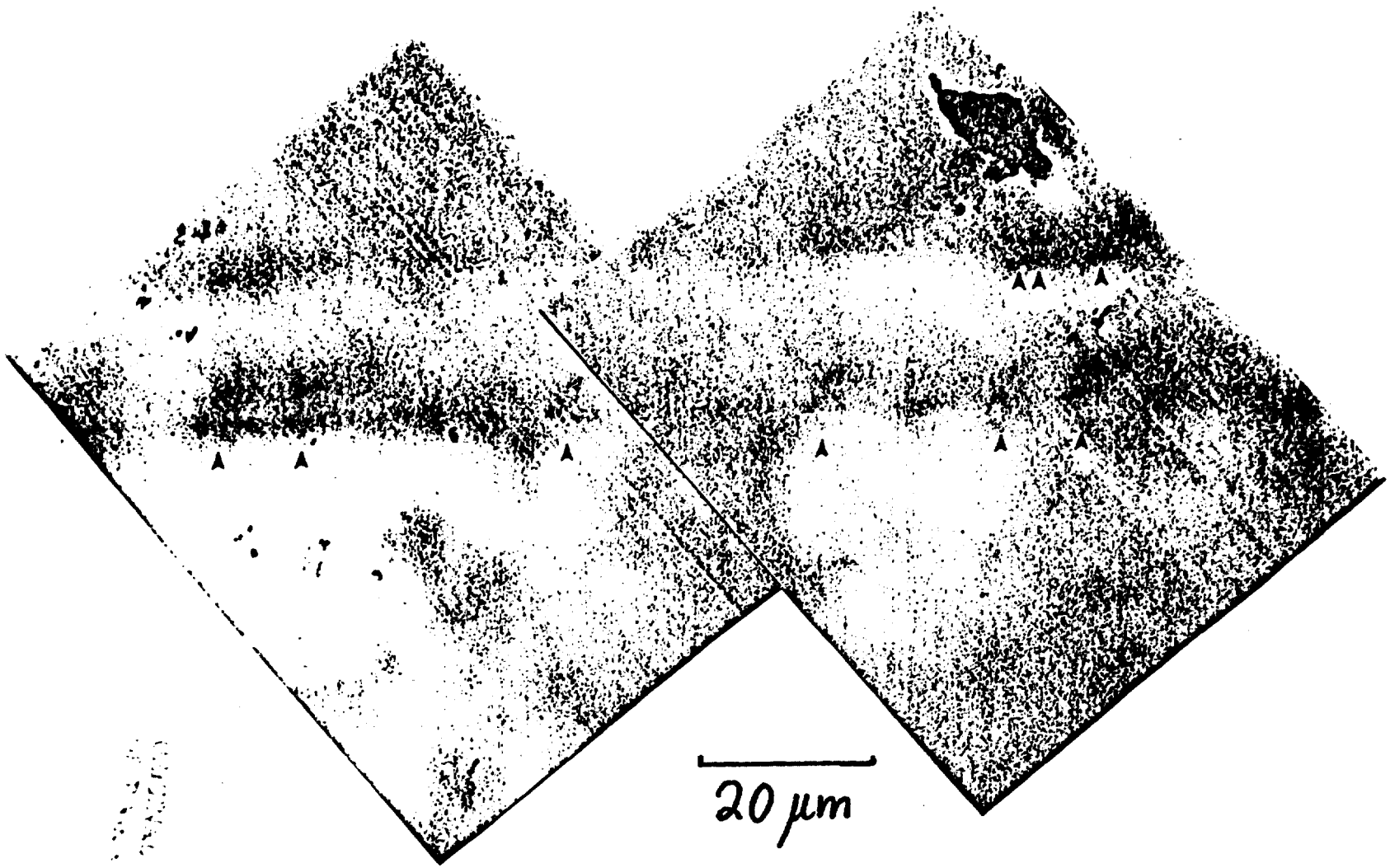

Figure 7